Trajectory Tracking Control for a Quadcopter under External Disturbances

Cuong V. Nguyen
Thai Nguyen University of Information and Communication Technology, Thai Nguyen University, Vietnam
nvcuong@ictu.edu.vn

Minh Tuan Nguyen
Thai Nguyen University of Technology, Thai Nguyen University, Vietnam
nguyentuanminh@tnut.edu.vn (corresponding author)

Hoang. T. Tran
Center of Electrical Engineering, Duy Tan University, Danang, 550000, Vietnam
tranthuanhoang@duytan.edu.vn

Mien L. Trinh
University of Transport and Communications, Ha Noi 100000, Vietnam
mientl@utc.edu.vn

Hung M. La
University of Nevada, Reno, 1664 North Virginia Street, MS0171, Reno, 89557, NV, USA
hla@unr.edu

Hoa T. T. Nguyen
Thai Nguyen University of Technology, Thai Nguyen University, Vietnam
nguyenthituyethoa@tnut.edu.vn

Received: 21 July 2024 | Revised: 26 August 2024 | Accepted: 3 September 2024

 DOI: https://doi.org/10.48084/etasr.8449

ABSTRACT

This paper initially discusses the application of a Sliding Mode Controller (SMC) for drone control, encompassing vertical takeoff and landing. Subsequently, the dynamic model of the quadcopter is formulated using the Newton-Euler method. Despite the challenges posed by the nonlinear characteristics of Unmanned Aerial Vehicles (UAVs), empirical evidence from previous tests and simulation studies underscores the efficacy of the SMC in delivering satisfactory performance and robust resistance against interference. Moreover, this research endeavors to present a quadcopter model and simulation, leveraging the SMC alongside the Newton-Euler formula to enhance control precision in the face of external magnetic disturbances affecting the UAV. Both the position and attitude of the UAV are governed by the SMC. The dynamic and control models of the quadcopter are implemented and visualized in MATLAB, culminating in results that substantiate the efficacy of the proposed controller across diverse scenarios. Furthermore, the performance of the proposed control method is compared with alternative methodologies such as PID, particularly in scenarios involving disturbances. The simulation results indicate promising and practical implications.

Keywords-sliding mode control; UAV; backstepping; quadcopter; MATLAB/Simulink

I. INTRODUCTION

The research on Unmanned Aerial Vehicles (UAVs) for civil or military applications has promoted the need to operate these systems with higher requirements. The UAVs have shown versatility and efficiency in various fields such as Search And Rescue (SAR), meteorological research, infrastructure testing, homeland security, and traffic

monitoring, and precision agriculture. Quadcopters are widely utilized due to their convenience and flexibility in narrow operating ranges. They can fly in low areas, hover, and provide detailed information about that area through the control station. Many different controllers of quadcopters have been proposed, such as the Proportional Integral Derivative (PID) and Fuzzy control[1-4], Linear Quadratic Regulator/Gausian (LQR/G) [5], Sliding Mode Control (SMC) with LQR/G, SMC, backstepping control, adaptive control, optimal control, robust control, intelligent control, etc. to control position, altitude, and Euler angles [6].

The quadcopters have strong nonlinear properties and are affected by many external factors when operating. PID-based trajectory tracking control for quadcopters is an easy to implement method with low computational load. Still, it is difficult to determine the appropriate parameters K_p, K_i, and K_d (due to the need for an accurate quadcopter model). The PID controller reacts poorly to rapid changes, such as wind and aerodynamic disturbances. If strong winds or strong external forces act on the quadcopter, the PID controller may not be able to maintain the trajectory and may even increase oscillations and instability. Today's research often combines PID with other control methods, such as model predictive or robust control, to improve efficiency and meet more stringent requirements for quadcopter control under various disturbance conditions [6-10]. Backstepping control is a recursive algorithm that divides the controller into steps and gradually stabilizes each subsystem. The advantage of this algorithm is that the convergence is fast, resulting in a small amount of computations, and it can control disturbances well. The most significant limitation of this algorithm is its poor robustness. The backstepping approach is applied in [11-12] for the postural stabilization of a quadcopter. Thanks to its ability to obtain a fast output control response to the uncertainty of the input signal, SMC has become one of the most popular control methods for quadcopters. Authors in [13-14] presented a sliding controller to control the slope of a quadcopter. The quadcopter system is divided into two position and attitude subsystems. Sliding controller integrated with Radial Basis Function Neural Network (RBFNN) ensures faster convergence of state variables to their desired values in short time [15-17]. A sliding controller hybrid with a backstepping controller for position tracking of the quadcopter is proposed in [18-19]. When using a PID controller is applied to control the position of the quadcopter, as in [13], may lead to huge errors when a disturbance is acting on the quadcopter. Most relevant studies do not mention when the system is affected by external disturbances. Adaptive control is a control method that can self-adjust the controller parameters to adapt to rapid changes in the flight environment, such as changes in altitude, wind speed, or mass of the quadcopter and complex and variable environmental conditions. Adaptive control can minimize errors and improve the accuracy of the quadcopter in maintaining its position and flight direction due to its ability to continuously adjust the control parameters over time to ensure the stability and trajectory tracking of the quadcopter. The disadvantage of this method is that it has a more complex design than traditional control methods such as PID and LQR. In some cases, adaptive control can lead to instability of the quadcopter during flight if the controller is not designed and adjusted correctly, and slow response may occur in complex flight environments [20-22].

In this paper, an advanced SMC is proposed based on Lyapunov stability theory for position control and attitude control of the quadcopter taking into account as input the external disturbances. The simulation results will compare the case when there is no external disturbance and when there are many external disturbances to see the performance of the proposed controller. In this study, we design a control law to ensure the system's stability and track the trajectory of the quadcopter when there are unknown parameters, such as the moment of inertia and external force. The contribution of this paper is briefly described by the following points:

- A full quadcopter mathematical model built with external disturbances is proposed.
- A solution to overcome the chattering phenomenon in conventional SMC is proposed.
- The control quality of the proposed SMC method is compared to the PID method during experimental implementation.

II. KINETIC MODEL OF THE QUADCOPTER

The structural model of the quadcopter and the coordinate systems used in building the dynamics model of the quadcopter are shown in Figure 1. The reference system associated with the earth is the $O_E x_E y_E z_E$ coordinate system, and the reference system associated with the quadcopter is the $O_B\ x_B\ y_B\ z_B$ coordinate system. The origin is chosen to coincide with the quadcopter's centroid. F_i, M_i, Ω_i are the respective forces, torques, and speeds generated from the propeller blades [23].

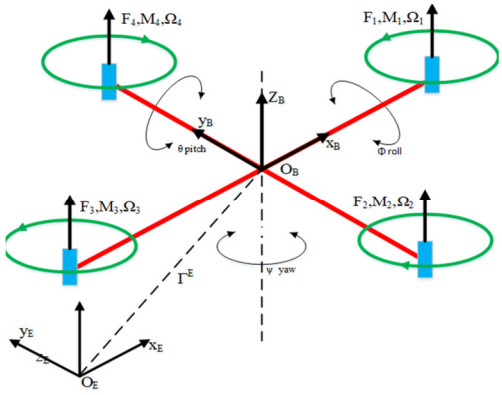

Fig. 1. Structural model of the quadcopter.

Using the Newton - Euler method for the UAV model, we get the quadcopter's equations of motion as follows:

$$\begin{cases} m\ddot{\Gamma}^E = F_{th} - F_d - F_g - F_n \\ I\ddot{\Theta}^E = M - M_{gp} - M_{gb} - M_n \end{cases} \quad (2.1)$$

where $F_{th} = R_\Theta(\phi, \theta, \psi)[0,0\sum_{i=1}^{4} F_i]^T$ is the total thrust of the four propellers; $F_d = diag(k_1, k_2, k_3)\dot{\Gamma}^T$ is the air resistance against the quadcopter's motion; $F_g = [0,\ 0,\ mg]^T$ is the force of

gravity; F_n is the total resistance of the noise types not included in the above components; m is the drone's mass; g is the acceleration due to gravity; $M = [M_\phi, M_\theta, M_\psi]^T$ is the sum of the moments of the roll, pitch, and yaw angles; M_{gp} and M_{gb} are the gyroscope moments; M_n is the resisting moment component of the disturbance.

Substituting the position vector and force components into (2.1), we get the quadcopter's translational dynamics equation as follows:

$$\begin{cases} \ddot{x} = -\frac{k_x}{m}\dot{x} + (cos\emptyset sin\theta cos\psi + sin\emptyset sin\psi)\frac{U_1}{m} - \frac{F_{nx}}{m} \\ \ddot{y} = -\frac{k_y}{m}\dot{y} + (cos\emptyset sin\theta sin\psi + sin\emptyset cos\psi)\frac{U_1}{m} - \frac{F_{ny}}{m} \\ \ddot{z} = -\frac{k_z}{m}\dot{z} - g + (cos\emptyset cos\theta)\frac{U_1}{m} - \frac{F_{nz}}{m} \end{cases} \quad (2.2)$$

where F_{nx}, F_{ny}, F_{nz} are the repulsive forces of the disturbance in the x, y, and z directions.

Substituting the moment components into (2.1), we get the kinematics equation for the rotation of the quadcopter as follows:

$$\begin{cases} \ddot{\emptyset} = \dot{\theta}\dot{\psi}\frac{I_y - I_z}{I_x} - \frac{J_p}{I_x}\Omega_\Sigma\dot{\theta} + lb\frac{U_2}{I_x} - \frac{M_{n\emptyset}}{I_x} \\ \ddot{\theta} = \dot{\emptyset}\dot{\psi}\frac{I_z - I_x}{I_y} + \frac{J_p}{I_y}\Omega_\Sigma\dot{\emptyset} + lb\frac{U_3}{I_y} - \frac{M_{n\theta}}{I_y} \\ \ddot{\psi} = \dot{\emptyset}\dot{\theta}\frac{I_x - I_y}{I_z} + d\frac{U_4}{I_z} - \frac{M_{n\psi}}{I_z} \end{cases} \quad (2.3)$$

where $\Omega_\Sigma = \Omega_1 - \Omega_2 + \Omega_3 - \Omega_4$ is the total speed of the propellers; $M_{n\emptyset}$, $M_{n\theta}$, and $M_{n\psi}$ are the resisting moment components of the disturbance acting on the roll, pitch, and yaw angles.

We let $X^T = (x, y, z, \dot{x}, \dot{y}, \dot{z}, \phi, \theta, \psi, \dot{\phi}, \dot{\theta}, \dot{\psi})^T$ be the vector of state variables. $x_1 = \phi$; $x_2 = \dot{\phi}$; $x_3 = \theta$; $x_4 = \dot{\theta}$; $x_5 = \psi$; $x_6 = \dot{\psi}$; $x_7 = x$; $x_8 = \dot{x}$; $x_9 = y$; $x_{10} = \dot{y}$; $x_{11} = z$; $x_{12} = \dot{z}$. The equation of state describing the kinematics of the quadcopter has the following form:

$\dot{X} = f(X,U) =$

$$\begin{cases} \dot{x}_1 = x_2 \\ \dot{x}_2 = -\frac{k_x}{m}\dot{x} + (cos\emptyset sin\theta cos\psi + sin\emptyset sin\psi)\frac{U_1}{m} - \frac{F_{nx}}{m} \\ \dot{x}_3 = x_4 \\ \dot{x}_4 = -\frac{k_y}{m}\dot{y} + (cos\emptyset sin\theta sin\psi + sin\emptyset cos\psi)\frac{U_1}{m} - \frac{F_{ny}}{m} \\ \dot{x}_5 = x_6 \\ \dot{x}_6 = -\frac{k_z}{m}\dot{z} - g + (cos\emptyset cos\theta)\frac{U_1}{m} - \frac{F_{nz}}{m} \\ \dot{x}_7 = x_8 \\ \dot{x}_8 = \dot{\theta}\dot{\psi}\frac{I_y - I_z}{I_x} - \frac{J_p}{I_x}\Omega_\Sigma\dot{\theta} + lb\frac{U_2}{I_x} - \frac{M_{n\emptyset}}{I_x} \\ \dot{x}_9 = x_{10} \\ \dot{x}_{10} = \dot{\emptyset}\dot{\psi}\frac{I_z - I_x}{I_y} + \frac{J_p}{I_y}\Omega_\Sigma\dot{\emptyset} + lb\frac{U_3}{I_y} - \frac{M_{n\theta}}{I_y} \\ \dot{x}_{11} = x_{12} \\ \dot{x}_{12} = \dot{\emptyset}\dot{\theta}\frac{I_x - I_y}{I_z} + \frac{dU_4}{I_z} - \frac{M_{n\psi}}{I_z}. \end{cases} \quad (2.4)$$

From the system of state equations of the quadcopter (2.4) we set: $h_1 = -\frac{k_x}{m}; h_2 = -\frac{F_{nx}}{m}; h_3 = -\frac{k_y}{m}; h_4 = -\frac{F_{ny}}{m}; h_5 = -\frac{k_z}{m};$

$h_6 = -\frac{F_{nz}}{m};\ h_7 = \frac{I_y - I_z}{I_x};\ h_8 = -\frac{J_r}{I_x}\Omega_\Sigma;\ h_9 = \frac{1}{I_x}; h_{10} = -\frac{M_{n\emptyset}}{I_x};$

$h_{11} = \frac{I_z - I_x}{I_y};\ h_{12} = \frac{J_p}{I_y}\Omega_\Sigma;\ h_{13} = \frac{lb}{I_y}; h_{14} = -\frac{M_{n\theta}}{I_y};\ h_{15} = \frac{I_x - I_y}{I_z};$

$h_{16} = \frac{d}{I_z}; h_{17} = -\frac{M_{n\psi}}{I_z};\ U_x = \frac{U_1}{m}(cos\emptyset sin\theta cos\psi + sin\emptyset sin\psi);$

$\Omega_\Sigma = \omega_1 - \omega_2 + \omega_3 - \omega_4;$

$U_y = \frac{U_1}{m}(cos\emptyset sin\theta sin\psi + sin\emptyset cos\psi);$

$U_z = \frac{U_1}{m}(cos\emptyset cos\theta) - g;$

We have:

$$\dot{X} = f(X,U) = \begin{cases} \dot{x}_1 = x_2 \\ \dot{x}_2 = h_1 x_2 + h_2 + U_x \\ \dot{x}_3 = x_4 \\ \dot{x}_4 = h_3 x_4 + h_4 + U_y \\ \dot{x}_5 = x_6 \\ \dot{x}_6 = h_5 x_6 + h_6 + U_z \\ \dot{x}_7 = x_8 \\ \dot{x}_8 = h_7 x_{10} x_{12} + h_8 x_{10} + h_{10} + h_9 U_2 \\ \dot{x}_9 = x_{10} \\ \dot{x}_{10} = h_{11} x_8 x_{12} + h_{12} x_8 + h_{14} + h_{13} U_3 \\ \dot{x}_{11} = x_{10} \\ \dot{x}_{12} = h_{15} x_8 x_{10} + h_{17} + h_{16} U_4 \end{cases} \quad (2.5)$$

III. PROPOSED QUADCOPTER SMC CONTROLLER

In this section, we have built a control scheme to control the position and attitude of the quadcopter using SMC. Position and attitude controllers were constructed, and the stability of the proposed controller was proven.

A. Synthesizing Principle of the Quadcopter Controller

We can see that there are six output signal channels, including three position channels (x, y, and z) and three angle channels (roll, pitch, yaw). However, these channels are not independent but interdependent. The main dependencies are explained in detail below:

- X channel: When we want to control the quadcopter to fly along the X axis, we need to create a control signal to change the pitch angle (θ) corresponding to the speed (signal from block M2) while still creating lift force, generating signal U_1. The roll (ϕ) and yaw (ψ) angles will be kept at zero. After arriving at the new position, the pitch angle must also be returned to zero, and that value must be kept stable.
- Y channel: When we want to control the quadcopter to fly along the Y axis, we need to create a control signal to change the roll angle (ϕ) corresponding to the speed (signal from block M2), and at the same time still have to create lift force, that is, create U_1 signal. In this case, the pitch (θ) and yaw (ψ) angles will be kept stable at zero. After arriving at the new position, the roll angle must also be returned to zero, and that value must be kept stable.
- Z channel: When controlling altitude, we need to increase the speed of all four propeller motors (generate signal U_1).

In this case, the roll, pitch, and yaw angles will be kept constant at zero.

In Figure 2, the controllers for the posture loop include the roll and pitch channel controllers, whose set value depends on the *x*, *y*, and *z* length speed control channels. In contrast, the yaw angle controller is an independent controller. The U_1 signals will be synthesized and have a close relationship with the U4 signal of the yaw channel to control the *x*, *y*, and *z* channels while maintaining a stable yaw angle.

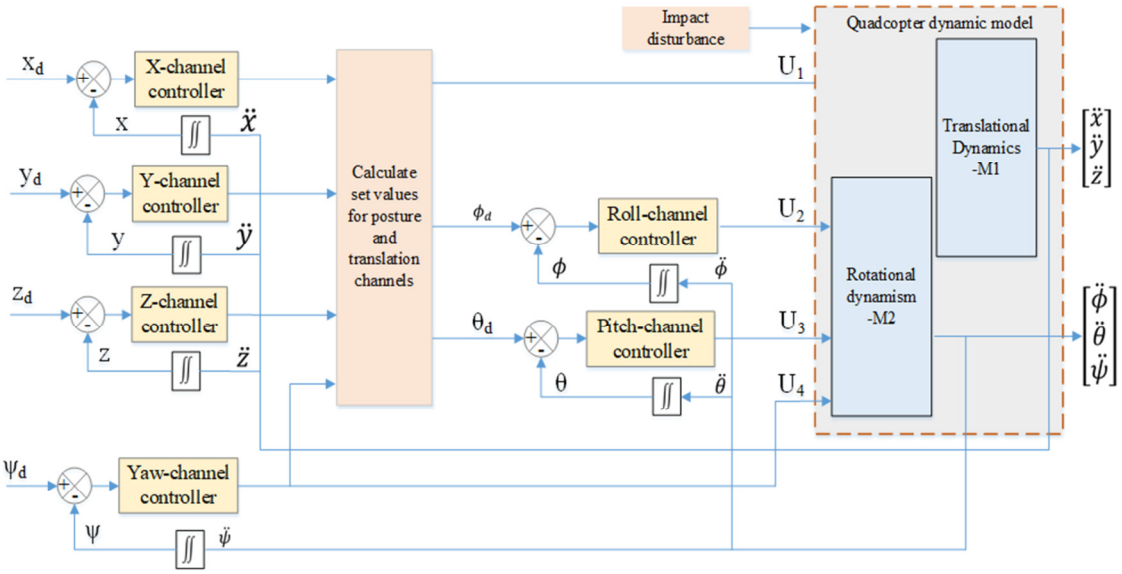

Fig. 2. Block diagram of the quadcopter channel control system.

B. *SMC design for Position Control of the Quadcopter*

We set the tracking error:

$$\begin{bmatrix} e_1 \\ e_3 \\ e_5 \end{bmatrix} = \begin{bmatrix} x_1 - x_{1d} \\ x_3 - x_{3d} \\ x_5 - x_{5d} \end{bmatrix} \Longrightarrow$$

$$\begin{bmatrix} \dot{e_1} \\ \dot{e_3} \\ \dot{e_5} \end{bmatrix} = \begin{bmatrix} \dot{x_1} - \dot{x_{1d}} \\ \dot{x_3} - \dot{x_{3d}} \\ \dot{x_5} - \dot{x_{5d}} \end{bmatrix} = \begin{bmatrix} x_2 - \dot{x_{1d}} \\ x_4 - \dot{x_{3d}} \\ x_6 - \dot{x_{5d}} \end{bmatrix} \quad (3.1)$$

The sliding surface is selected as follows:

$$s = \begin{bmatrix} s_1 \\ s_3 \\ s_5 \end{bmatrix} = \begin{bmatrix} c_1 e_1 + c_2 \dot{e_1} \\ c_3 e_3 + c_4 \dot{e_3} \\ c_5 e_5 + c_6 \dot{e_5} \end{bmatrix} \Longrightarrow \dot{s} = \begin{bmatrix} c_1 \dot{e_1} + c_2 \ddot{e_1} \\ c_3 \dot{e_3} + c_4 \ddot{e_3} \\ c_5 \dot{e_5} + c_6 \ddot{e_5} \end{bmatrix}$$

$$= \begin{bmatrix} c_1(x_2 - \dot{x_{1d}}) + c_2(\dot{x_2} - \ddot{x_{1d}}) \\ c_3(x_4 - \dot{x_{3d}}) + c_4(\dot{x_4} - \ddot{x_{3d}}) \\ c_5(x_6 - \dot{x_{5d}}) + c_6(\dot{x_6} - \ddot{x_{5d}}) \end{bmatrix} \quad (3.2)$$

Substituting $\dot{x_2}, \dot{x_4}, \dot{x_6}$ from (2.5) into (3.2), we have:

$$\dot{s} = \begin{bmatrix} c_1(x_2 - \dot{x_{1d}}) + c_2(h_1 x_2 + h_2 + U_x - \ddot{x_{1d}}) \\ c_3(x_4 - \dot{x_{3d}}) + c_4(h_3 x_4 + h_4 + U_y - \ddot{x_{3d}}) \\ c_5(x_6 - \dot{x_{5d}}) + c_6(h_5 x_6 + h_6 + U_z - \ddot{x_{5d}}) \end{bmatrix} \quad (3.3)$$

In the SMC there are two components, which are equilibrium and robust terms:

$$u = u_{EQ} + u_R \quad (3.4)$$

The equilibrium component will be selected by setting the sliding surface's derivative $\dot{s} = -ks$ and giving the system's uncertainty parameter = 0. Then we have:

$$u_{EQ} = \begin{bmatrix} u_{EQx} \\ u_{EQy} \\ u_{EQz} \end{bmatrix} =$$

$$\begin{bmatrix} \frac{1}{c_2}(-c_1(x_2 - \dot{x_{1d}}) - c_2(h_1 x_2 - \ddot{x_{1d}}) - k_1 s_1) \\ \frac{1}{c_4}(-c_3(x_4 - \dot{x_{3d}}) - c_4(h_3 x_4 - \ddot{x_{3d}}) - k_3 s_3) \\ \frac{1}{c_6}(-c_5(x_6 - \dot{x_{5d}}) + c_6(h_5 x_6 - \ddot{x_{5d}}) - k_5 s_5) \end{bmatrix} \quad (3.5)$$

The robust component will be chosen as $u_R = -\eta sign(s)$, so we have:

$$u_R = \begin{bmatrix} u_{Rx} \\ u_{Ry} \\ u_{Rz} \end{bmatrix} = \begin{bmatrix} -\frac{1}{c_2}(\eta_1 sign(s_1)) \\ -\frac{1}{c_4}(\eta_3 sign(s_3)) \\ -\frac{1}{c_6}(\eta_5 sign(s_5)) \end{bmatrix} \quad (3.6)$$

η is chosen such that it is equal or greater than the maximum value of the uncertain parameters in the system.

Substituting $u_{EQ}; u_R$ into (3.4) we have:

$$\begin{bmatrix} U_x \\ U_y \\ U_z \end{bmatrix} =$$

$$\begin{bmatrix} \frac{1}{c_2}(-c_1(x_2 - \dot{x_{1d}}) - c_2(h_1x_2 - \ddot{x_{1d}}) - k_1s_1 - \eta_1 sign(s_1)) \\ \frac{1}{c_4}(-c_3(x_4 - \dot{x_{3d}}) - c_4(h_3x_4 - \ddot{x_{3d}}) - k_3s_3 - \eta_3 sign(s_3)) \\ \frac{1}{c_6}(-c_5(x_6 - \dot{x_{5d}}) + c_6(h_5x_6 - \ddot{x_{5d}}) - k_5s_5 - \eta_5 sign(s_5)) \end{bmatrix} \quad (3.7)$$

After obtaining the control signals U_x, U_y, U_z we calculate the control signal U_1 in the system as follows:

$$U_1 = m\sqrt{U_x^2 + U_y^2 + (U_z + g)^2} \quad (3.8)$$

C. Proof of the Stability of the Controlled System

Substituting the SMC rule in (3.7) into (3.3), we have:

$$\dot{s} = \begin{bmatrix} \dot{s_1} \\ \dot{s_3} \\ \dot{s_5} \end{bmatrix} = \begin{bmatrix} -k_1s_1 - \eta_1 sign(s_1) + h_2 \\ -k_3s_3 - \eta_3 sign(s_3) + h_4 \\ -k_5s_5 - \eta_5 sign(s_5) + h_6 \end{bmatrix} \quad (3.9)$$

To prove the stability of the control system, the positive definite Lyapunov function is chosen as follows:

$$v = \begin{bmatrix} v_1 \\ v_3 \\ v_5 \end{bmatrix} = \begin{bmatrix} \frac{1}{2}s_1^2 \\ \frac{1}{2}s_3^2 \\ \frac{1}{2}s_5^2 \end{bmatrix} \quad (3.10)$$

Calculating the derivative v, we have:

$$\begin{bmatrix} \dot{v_1} \\ \dot{v_3} \\ \dot{v_5} \end{bmatrix} = \begin{bmatrix} s_1\dot{s_1} \\ s_3\dot{s_3} \\ s_5\dot{s_5} \end{bmatrix} = \begin{bmatrix} s_1(-k_1s_1 - \eta_1 sign(s_1) + h_2) \\ s_3(-k_3s_3 - \eta_3 sign(s_3) + h_4) \\ s_5(-k_5s_5 - \eta_5 sign(s_5) + h_6) \end{bmatrix} \quad (3.11)$$

$$\begin{bmatrix} \dot{v_1} \\ \dot{v_3} \\ \dot{v_5} \end{bmatrix} = \begin{bmatrix} -k_1s_1^2 - s_1(\eta_1 sign(s_1) - h_2) \\ -k_3s_3^2 - s_3(\eta_3 sign(s_3) - h_4) \\ -k_5s_5^2 - s_5(\eta_5 sign(s_5) - h_6) \end{bmatrix} \quad (3.12)$$

We have:

$$\begin{bmatrix} -k_1s_1^2 - s_1(\eta_1 sign(s_1) - h_2) \\ -k_3s_3^2 - s_3(\eta_3 sign(s_3) - h_4) \\ -k_5s_5^2 - s_5(\eta_5 sign(s_5) - h_6) \end{bmatrix} \leq \begin{bmatrix} -k_1s_1^2 - |s_1|(\eta_1 - h_2) \\ -k_3s_3^2 - |s_3|(\eta_3 - h_4) \\ -k_5s_5^2 - |s_5|(\eta_5 - h_6) \end{bmatrix} \leq \begin{bmatrix} -k_1s_1^2 \\ -k_3s_3^2 \\ -k_5s_5^2 \end{bmatrix} \leq 0;$$

since we have the condition η. The η is chosen so that $\eta \geq$ the maximum value of the uncertain parameters in the system. Therefore, according to the Lyapunov stability theory, the system is stable.

D. SMC Design for the Attitude Control of the Quadcopter

We set the tracking error:

$$\begin{bmatrix} e_7 \\ e_9 \\ e_{11} \end{bmatrix} = \begin{bmatrix} x_7 - x_{7d} \\ x_9 - x_{9d} \\ x_{11} - x_{11d} \end{bmatrix}$$

$$\Rightarrow \begin{bmatrix} \dot{e_7} \\ \dot{e_9} \\ \dot{e_{11}} \end{bmatrix} = \begin{bmatrix} \dot{x_7} - \dot{x_{7d}} \\ \dot{x_9} - \dot{x_{9d}} \\ \dot{x_{11}} - \dot{x_{11d}} \end{bmatrix} = \begin{bmatrix} x_8 - \dot{x_{7d}} \\ x_{10} - \dot{x_{9d}} \\ x_{12} - \dot{x_{11d}} \end{bmatrix} \quad (3.13)$$

The calculation process is similar to the one above. We have:

$$\begin{bmatrix} U_2 \\ U_3 \\ U_4 \end{bmatrix} =$$

$$\begin{bmatrix} \frac{1}{c_8h_9}[-c_7(x_8 - \dot{x_{7d}}) - c_8(h_7x_{10}x_{12} + h_8x_{10} - \ddot{x_{7d}}) \\ -k_7s_7 - \eta_7 sign(s_7)] \\ \frac{1}{c_{10}h_{13}}[-c_9(x_{10} - \dot{x_{9d}}) - c_{10}(h_{11}x_8x_{12} + h_{12}x_8 - \ddot{x_{9d}}) \\ -k_9s_9 - \eta_9 sign(s_9)] \\ \frac{1}{c_{12}h_{16}}[-c_{11}(x_{12} - \dot{x_{11d}}) - c_{12}(h_{15}x_8x_{10} - \ddot{x_{11d}}) \\ -k_{11}s_{11} - \eta_{11} sign(s_{11})] \end{bmatrix} \quad (3.14)$$

The process of proving the stability of the system is performed similarly as above.

IV. SIMULATION AND EXPERIMENTAL RESULTS

A. Reducing the Chattering Phenomenon

SMC has several advantages: robustness against uncertainties and disturbances, high accuracy, finite-time convergence, and simplicity. However, it has the disadvantage of the chattering phenomenon because it uses the sign(s) function in the control signal. Therefore, we need to devise a solution to overcome this phenomenon. In this study, we replace the sign(s) function with $|s|^{\lambda}$sign(s). The simulation results in Figure 3 demonstrate the effectiveness of this solution. In similar paper [24], the authors mentioned external disturbances in building a kinematic model of the quadcopter. However, they assume that all external disturbances are zero when performing simulations. Thus, we will not clearly see the nature and outstanding advantages of the SMC. In addition, in [24], the authors did not mention the chattering phenomenon in sliding control and how to overcome it. We overcome both these limitations this study. External disturbances were considered and solutions to reduce the chattering phenomenon in the SMC were provided. Equations (3.7) and (3.14) are rewritten as:

$$\begin{bmatrix} U_x \\ U_y \\ U_z \end{bmatrix} = \begin{bmatrix} \frac{1}{c_2}(-c_1(x_2 - \dot{x_{1d}}) - c_2(h_1x_2 - \ddot{x_{1d}}) \\ -k_1s_1 - \eta_1|s_1|^{\lambda} sign(s_1)) \\ \frac{1}{c_4}(-c_3(x_4 - \dot{x_{3d}}) - c_4(h_3x_4 - \ddot{x_{3d}}) \\ -k_3s_3 - \eta_3|s_3|^{\lambda} sign(s_3)) \\ \frac{1}{c_6}(-c_5(x_6 - \dot{x_{5d}}) + c_6(h_5x_6 - \ddot{x_{5d}}) \\ -k_5s_5 - \eta_5|s_5|^{\lambda} sign(s_5)) \end{bmatrix} \quad (4.1)$$

$$\begin{bmatrix} U_2 \\ U_3 \\ U_4 \end{bmatrix} = \begin{bmatrix} \frac{1}{c_8h_9}[-c_7(x_8 - \dot{x_{7d}}) - c_8(h_7x_{10}x_{12} \\ +h_8x_{10} - \ddot{x_{7d}}) - k_7s_7 - \eta_7|s_7|^{\lambda} sign(s_7)] \\ \frac{1}{c_{10}h_{13}}[-c_9(x_{10} - \dot{x_{9d}}) - c_{10}(h_{11}x_8x_{12} \\ +h_{12}x_8 - \ddot{x_{9d}}) - k_9s_9 - \eta_9|s_9|^{\lambda} sign(s_9)] \\ \frac{1}{c_{12}h_{16}}[-c_{11}(x_{12} - \dot{x_{11d}}) - c_{12}(h_{15}x_8x_{10} \\ -\ddot{x_{11d}}) - k_{11}s_{11} - \eta_{11}|s_{11}|^{\lambda} sign(s_{11})] \end{bmatrix} \quad (4.2)$$

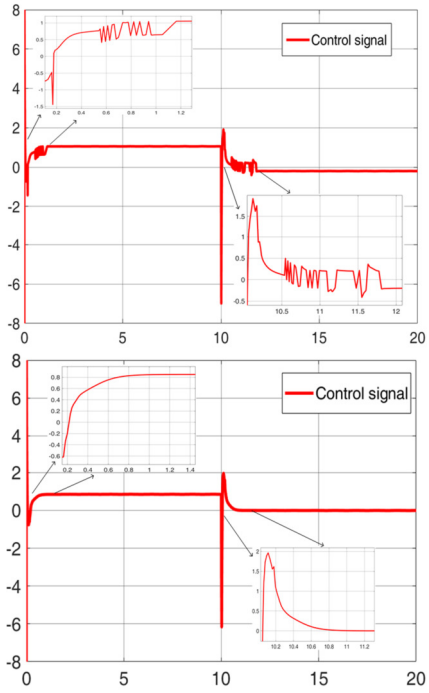

Fig. 3. Solution for chattering phenomenon.

Numerical simulations are presented in this section to exhibit the proposed controllers' effectiveness. The parameters of the Quadcopter used in the simulation are given in Table I. Parameters are assumed according to the parameters of the real quadcopter. The time the system moves towards the sliding surface depends on the coefficient η. The larger the η, the faster the time of the sliding surface, but this causes a larger chattering phenomenon. To ensure that the time of moving towards the sliding surface is both fast and does not have the chattering phenomenon, we propose to add the coefficient $|s|^{\lambda}$ so that when the system moves towards the sliding surface, the variable $|s|$ will approach 0. At that time, $\eta.|s|^{\lambda}$ is zero, so the chattering phenomenon is eliminated.

TABLE I. PARAMETERS USED IN SIMULATIONS

Parameter	Value	Parameter	Value
m (kg)	1.1	b (N.s^2)	6.6231.10^{-6}
g (m/s^2)	9.81	d (N.m/s^2)	0.3512.10^{-6}
I_x (kg.m^2)	0.0225	l (m)	0.2
I_y (kg.m^2)	0.0225	k_x (N/m/s)	5.657 e^{-4}
I_z (kg.m^2)	0.0452	k$_y$ (N/m/s)	5.657 e^{-4}
J_p(kg.m^2)	7.5.10^{-4}	k_z (N/m/s)	6.261 e^{-5}

To best evaluate the effectiveness of the designed controller, the quadcopter flew along two different trajectories, without and with noise, as shown in Figure 4 and Figure 8. Simulation results demonstrate that the proposed controller can operate effectively across various trajectories, yielding good control performance. The two considered trajectories are both fairly complex and exist in practical scenarios. In the ideal case without interference, we see that the proposed control algorithm has very good trajectory tracking control quality. Even if the UAV's initial position is not in the desired orbit, the UAV can move to the desired orbit after a short period as shown in Figures 5-6. When flying the quadcopter along the second trajectory, excellent trajectory tracking quality is demonstrated, as shown in Figure 7.

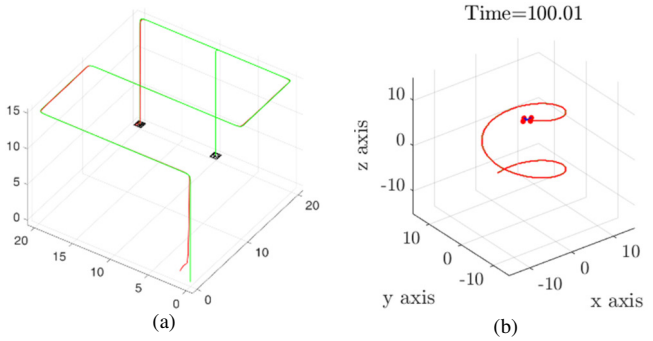

Fig. 4. 3D simulation model without noise. (a) First trajectory, (b) second trajectory.

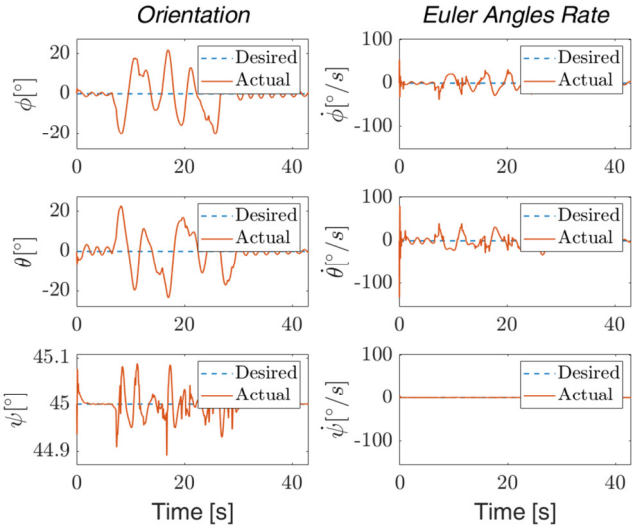

Fig. 5. Orientation vs time without noise for the first trajectory.

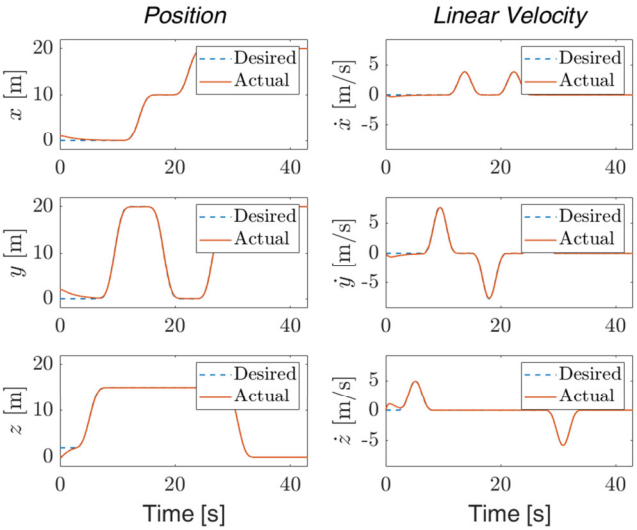

Fig. 6. Position vs time without noise for the first trajectory.

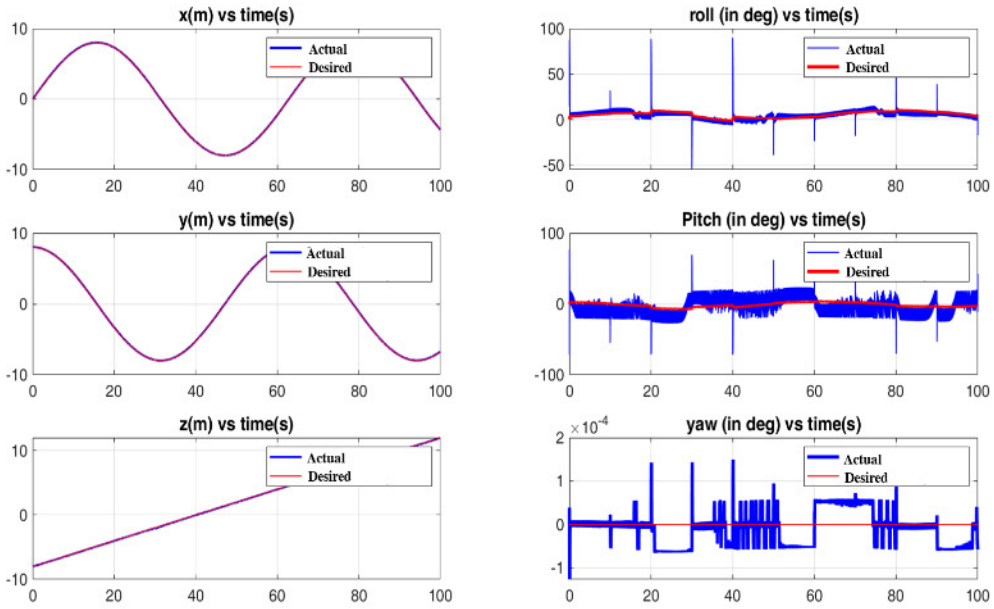

Fig. 7. Position and orientation vs time without noise for the second trajectory.

In the second scenario, external disturbances affecting the UAV were considered.

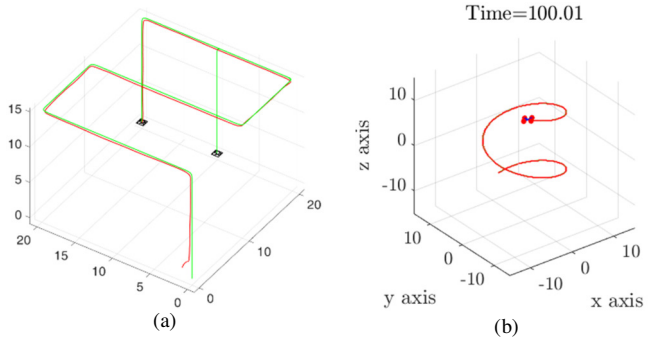

Fig. 8. 3D simulation model with noise. (a) First trajectory, (b) second trajectory.

The simulation results in Figures 8-10 show that the trajectory tracking control quality of the proposed algorithm is still very good. When disturbances occur at various time points, the proposed controller assists the quadcopter in quickly returning to the desired trajectory after being perturbed and deviating from its path, as indicated in Figure 11.

B. Experimental Results

To experimentally verify the control algorithm, we tested the F450 quadcopter's ability to fly according to a given trajectory automatically in a real environment. The parameters of quadcopter F450 are given in Table II. Figure 12 shows the desired flight trajectory in a space with dimensions of 20 m width, 20 m length, and 15 m height.

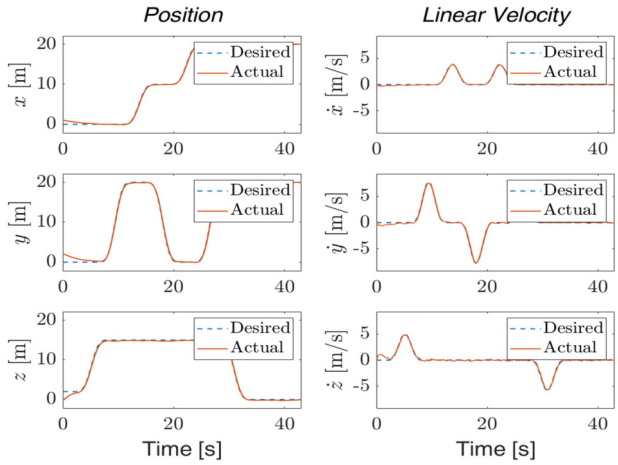

Fig. 9. Position vs time with noise following the first trajectory.

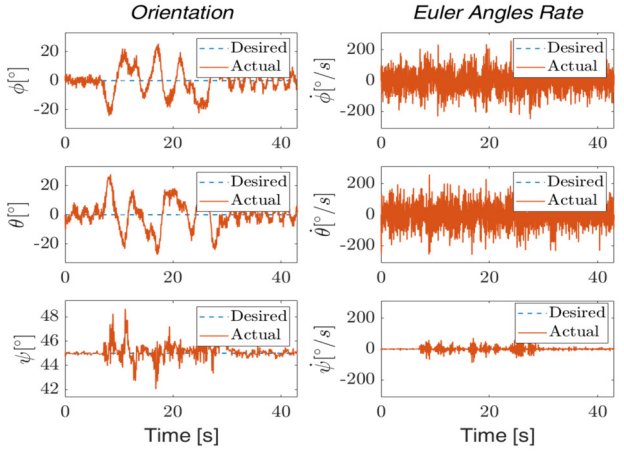

Fig. 10. Orientation vs time with noise following the first trajectory.

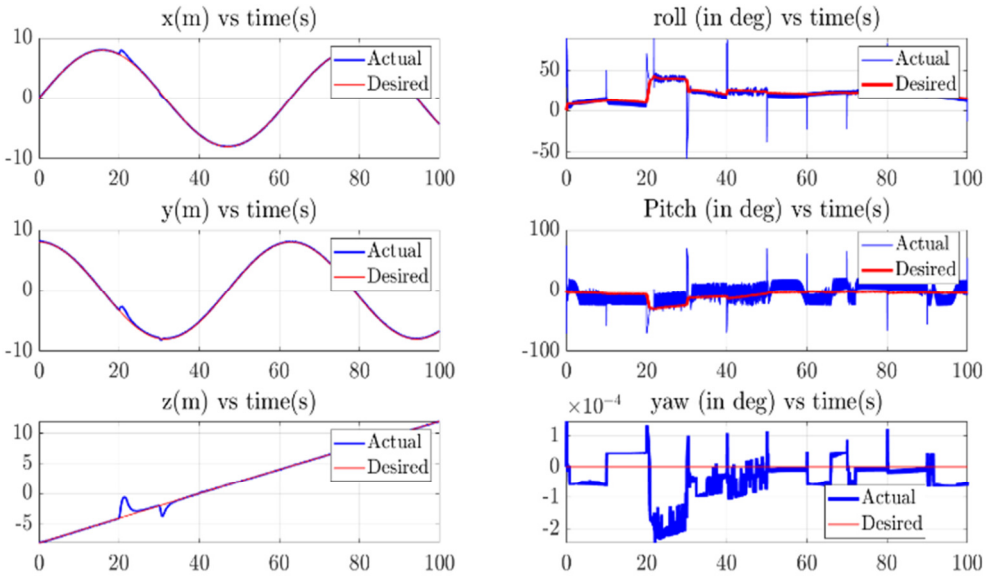

Fig. 11. Position and orientation vs time with noise for the second trajectory.

TABLE II. ACTUAL QUADCOPTER PARAMETERS

Parameter	Values
Mass	1.1 kg
Maximum current per motor	I_{motor} = 4.28 A
Current of other loads on the UAV	I_{other} = 6.2 A
Serial cell number in PIN	N_{series} = 3s Cell
Nominal voltage of the PIN	$V_{bat\ nominal}$ = 11.1 V
Battery capacity	Q = 4200 mmAh
Battery C-rate	C_{rate} = 10
Battery discharge rule	DR = 80 %
Flying load	L_{flying} = 30 %

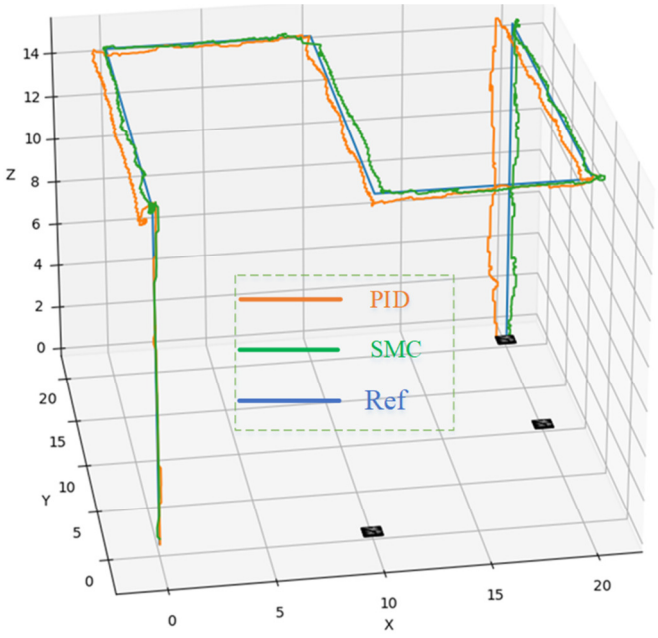

Fig. 12. The desired flight trajectory of the quadcopter, the trajectory of the quadcopter when controlled by PID, and when controlled by the SMC.

The test scenario with the flight trajectory in Figure 12 is as follows: from the starting point, the quadcopter flies vertically to a height of 15 m at a speed of 2.05 m/s (E1), then maintains the same altitude and x direction, flies forward in the y direction for 20 m at a speed of 1.01 m/s (E2); then maintains the same altitude and y direction, flies forward in the x direction for 10 m at a speed of 1.01 m/s (E3); then maintains the same altitude and x direction, flies back in the y direction for 20 m at a speed of 1.21 m/s (E4); then maintains the same altitude and y direction, flies forward in the x direction for 10 m at a speed of 0.73 m/s (E5); then maintains the same altitude and x direction, flies forward in the y direction for 20 m at a speed of 1.21 1m/s (E6); and finally keeps x and y directions constant and lands at 0.59 m/s (E7). The quadcopter flight processes in stages from E1 to E7 are shown in Table III along with the maximum trajectory tracking error in the x, y, and z directions. From Table III, we can see that the maximum trajectory tracking error in general in all directions of the SMC is always less than or equal to that of the PID controller.

TABLE III. SUMMARY TABLE OF ERRORS IN DIFFERENT DIRECTION DURING THE QUADCOPTER TEST FLIGHT

Stage	Error_x(m)		Error_y(m)		Error_z(m)	
	PID	SMC	PID	SMC	PID	SMC
E1(z)	0.15	0.15	1.75	0.5	2	1.5
E2(y)	0.75	0.4	1.5	1.0	0.1	0.1
E3(x)	0.75	0.1	0.75	0.75	0.1	0.1
E4(y)	0.5	0.5	1.0	0.75	0.1	0.1
E5(x)	1.75	0.75	2.0	1.4	0.1	0.1
E6(y)	0.5	0.25	2.0	1.6	0.1	0.1
E7(z)	0.75	0.5	1.0	0.5	3	0.6

V. CONCLUSIONS

In this paper, the use of a SMC to control position and attitude of the quadcopter has been successfully implemented. First, Newton-Euler equations were used to build the mathematical models for control design. The proposed SMC is

designed based on the Lyapunov function, so the system's stability is guaranteed. Finally, the proposed control scheme was applied to an autonomous flying quadcopter. The simulation results show that tracking responses with minor errors can be achieved with the proposed control system. In addition, this work also considers the impact of external disturbances to see the effectiveness of the proposed controller. Our results overcome existing work and show significant improvement. Besides, the proposed algorithm has been tested experimentally, showing its performance when applied in practice. Regarding future work, more investigation will be conducted to determine ways to create a sliding surface that can successfully account for time delay and provide a stable system.

ACKNOWLEDGMENTS

The authors would like to thank University of Transport and Communications, Thai Nguyen University of Technology, Thai Nguyen University, Vietnam Ministry of Education and Training (Project B2023-GHA-01) for the support.

REFERENCES

[1] A. Katiar, R. Rashdi, Z. Ali, and U. Baig, "Control and stability analysis of quadcopter," in *International Conference on Computing, Mathematics and Engineering Technologies*, Sukkur, Pakistan, Mar. 2018, pp. 1–6, https://doi.org/10.1109/ICOMET.2018.8346419.

[2] D. L. T. Tran, H. T. Do, H. T. Tran, T. Hoang, and M. T. Nguyen, "A Design and Implement of Fuzzy Controller for Taking-off and Landing for Unmanned Aerial Vehicles," in *International Conference on Engineering Research and Applications*, Thai Nguyen, Vietnam, Dec. 2022, pp. 13–22, https://doi.org/10.1007/978-3-031-22200-9_2.

[3] A. Noordin, M. A. M. Basri, and Z. Mohamed, "Simulation and experimental study on PID control of a quadrotor MAV with perturbation," *Bulletin of Electrical Engineering and Informatics*, vol. 9, no. 5, pp. 1811–1818, Oct. 2020, https://doi.org/10.11591/eei.v9i5.2158.

[4] H. T. Tran, D. L. T. Tran, V. Q. Nguyen, H. T. Do, and M. T. Nguyen, "A Novel Framework of Modelling, Control, and Simulation for Autonomous Quadrotor UAVs Utilizing Arduino Mega," *Wireless Communications and Mobile Computing*, vol. 2022, no. 1, 2022, Art. no. 3044520, https://doi.org/10.1155/2022/3044520.

[5] E. Okyere, A. Bousbaine, G. T. Poyi, A. K. Joseph, and J. M. Andrade, "LQR controller design for quad-rotor helicopters," *The Journal of Engineering*, vol. 2019, no. 17, pp. 4003–4007, 2019, https://doi.org/10.1049/joe.2018.8126.

[6] M. Maaruf, M. S. Mahmoud, and A. Ma'arif, "A Survey of Control Methods for Quadrotor UAV," *International Journal of Robotics and Control Systems*, vol. 2, no. 4, pp. 652–665, Sep. 2022, https://doi.org/10.31763/ijrcs.v2i4.743.

[7] J. Zhang and L. Guo, "Theory and Design of PID Controller for Nonlinear Uncertain Systems," *IEEE Control Systems Letters*, vol. 3, no. 3, pp. 643–648, Jul. 2019, https://doi.org/10.1109/LCSYS.2019.2915306.

[8] R. P. Borase, D. K. Maghade, S. Y. Sondkar, and S. N. Pawar, "A review of PID control, tuning methods and applications," *International Journal of Dynamics and Control*, vol. 9, no. 2, pp. 818–827, Jun. 2021, https://doi.org/10.1007/s40435-020-00665-4.

[9] M. Rinaldi, S. Primatesta, and G. Guglieri, "A Comparative Study for Control of Quadrotor UAVs," *Applied Sciences*, vol. 13, no. 6, Jan. 2023, Art. no. 3464, https://doi.org/10.3390/app13063464.

[10] I. Lopez-Sanchez and J. Moreno-Valenzuela, "PID control of quadrotor UAVs: A survey," *Annual Reviews in Control*, vol. 56, Jan. 2023, Art. no. 100900, https://doi.org/10.1016/j.arcontrol.2023.100900.

[11] A. T. Nguyen, N. Xuan-Mung, and S.-K. Hong, "Quadcopter Adaptive Trajectory Tracking Control: A New Approach via Backstepping Technique," *Applied Sciences*, vol. 9, no. 18, Jan. 2019, Art. no. 3873, https://doi.org/10.3390/app9183873.

[12] Y. Fan, Y. Cao, and T. Li, "Adaptive integral backstepping control for trajectory tracking of a quadrotor," in *4th International Conference on Information, Cybernetics and Computational Social Systems*, Dalian, China, Jul. 2017, pp. 619–624, https://doi.org/10.1109/ICCSS.2017.8091489.

[13] H. L. N. N. Thanh and S. K. Hong, "Quadcopter Robust Adaptive Second Order Sliding Mode Control Based on PID Sliding Surface," *IEEE Access*, vol. 6, pp. 66850–66860, Jan. 2018, https://doi.org/10.1109/ACCESS.2018.2877795.

[14] A. Eltayeb, M. Rahmat, M. Eltoum, and M. Basri, "Robust Adaptive Sliding Mode Control Design for Quadrotor Unmanned Aerial Vehicle Trajectory Tracking," *International Journal of Computing and Digital Systems*, vol. 9, no. 2, pp. 249–257, Mar. 2020, https://doi.org/10.12785/ijcds/090210.

[15] H. Razmi and S. Afshinfar, "Neural network-based adaptive sliding mode control design for position and attitude control of a quadrotor UAV," *Aerospace Science and Technology*, vol. 91, pp. 12–27, Aug. 2019, https://doi.org/10.1016/j.ast.2019.04.055.

[16] M. Gulzar and A. N. Abubakar, "Adaptive Backstepping and Sliding Mode Control of a Quadroto." 2024, https://doi.org/10.21203/rs.3.rs-3841025/v1.

[17] D. Matouk, F. Abdessemed, O. Gherouat, and Y. Terchi, "Second-Order Sliding Mode for Position and Attitude Tracking Control of Quadcopter UAV: Super-Twisting Algorithm," *International Journal of Innovative Computing, Information and Control*, vol. 16, no. 1, pp. 29–43, 2020, https://doi.org/10.24507/ijicic.16.01.29.

[18] N. Hamdadou, H. Bouadi, N. Hebablia, and M. Yazid, "Stochastic Estimator Based Adaptive Sliding Mode Control for a Quadrotor in Rainy Flight Conditions," *Unmanned Systems*, vol. 12, no. 1, pp. 133–148, Jan. 2024, https://doi.org/10.1142/S2301385024500092.

[19] Y. Nettari, M. Labbadi, and S. Kurt, "Adaptive Backstepping Integral Sliding Mode Control Combined with Super-Twisting Algorithm For Nonlinear UAV Quadrotor System," *IFAC-PapersOnLine*, vol. 55, no. 12, pp. 264–269, Jan. 2022, https://doi.org/10.1016/j.ifacol.2022.07.322.

[20] M. Achtelik, T. Bierling, J. Wang, L. Hocht, and F. Holzapfel, *Adaptive Control of a Quadcopter in the Presence of large/complete Parameter Uncertainties*. St. Louis, MO, USA: American Institute of Aeronautics and Astronautics, 2011.

[21] R. I. Perez, G. R. Galvan, A. J. M. Vazquez, and D. L. Alabazares, "Attitude control of a quadcopter using adaptive control technique," in *Adaptive Robust Control Systems*, London, UK: IntechOpen, 2018.

[22] K. M. Thu and A. I. Gavrilov, "Designing and Modeling of Quadcopter Control System Using L1 Adaptive Control," *Procedia Computer Science*, vol. 103, pp. 528–535, Jan. 2017, https://doi.org/10.1016/j.procs.2017.01.046.

[23] A. Benghezal, A. Nemra, N. I. Bouaziz, and M. Tadjine, "New Robust Backstepping Attitude Control Approach Applied to Quanser 3 DOF Hover Quadrotor in the Case of Actuators Faults," *Unmanned Systems*, vol. 12, no. 1, pp. 3–17, Jan. 2024, https://doi.org/10.1142/S2301385024500018.

[24] R. Mohamed and A. Karaarslan, "Sliding Mode Control-Based Modeling and Simulation of a Quadcopter," *Journal of Engineering Research and Reports*, vol. 24, no. 3, pp. 32–41, Feb. 2023, https://doi.org/10.9734/JERR/2023/v24i3806.